Biochimica et Biophysica Acta, 936 (1988) 307–318
Elsevier

BBA 42875

Refined purification and further characterization of oxygen-evolving and Tris-treated Photosystem II particles from the thermophilic *Cyanobacterium synechococcus* sp.

J.P. Dekker [a,*], E.J. Boekema [b], H.T. Witt [a] and M. Rögner [a,**]

[a] *Max-Volmer-Institut für Biophysikalische und Physikalische Chemie, Technische Universität Berlin, Berlin and* [b] *Fritz-Haber-Institut der Max-Planck-Gesellschaft, Berlin (Germany)*

(Received 9 March 1988)
(Revised manuscript received 18 July 1988)

Key words: Photosystem II; HPLC; Electron microscopy; (*Synechococcus*)

Highly active, monomeric and dimeric Photosystem II complexes were purified from the thermophilic cyanobacterium *Synechococcus* sp. by two sucrose density gradients, and the size, shape and mass of these complexes have been estimated (Rögner, M., Dekker, J.P., Boekema, E.J. and Witt, H.T. (1987) FEBS Lett. 219, 207–311). (1) Further purification could be obtained by ion-exchange chromatography, by which the 300 kDa monomer could be separated into a highly active, O_2-evolving fraction, and a fraction without O_2-evolving capacity, which has lost its extrinsic 34 kDa protein. Both showed very high reaction center activities as measured by the photoreduction of the primary quinone acceptor, Q_A, at 320 nm, being up to one reaction center per 31 Chl *a* molecules. (2) Tris-treatment yielded homogeneous 300 kDa particles which had lost their extrinsic 34 kDa polypeptide. Electron microscopy of this complex revealed very similar dimensions compared to the oxygen-evolving 300 kDa particle, except that the smallest dimension was decreased from about 6.5 nm to about 5.8 nm. This difference is attributed to the missing extrinsic 33 kDa protein, and the smallest dimension is attributed to the distance across the membrane. (3) Experiments are presented, allowing an estimation for the contribution of detergent to the other dimensions being about 2×1.5 nm for dodecyl β-D-maltoside. This leads to dimensions, corrected for detergent size, of 12.3×7.5 nm for the monomeric form of PS II and 12×15.5 nm for the dimeric form. (4) From some extracts a 35 kDa, chlorophyll-binding complex could be isolated which lacks the characteristic absorbance changes of Q_A and of Chl a_{II} (P-680) and is therefore supposed to be a light-harvesting complex of cyanobacteria. (5) A model for the in vivo organization of PS II in cyanobacteria is discussed.

* Present address: Department of Biology, University of Michigan, Ann Arbor, MI, U.S.A.
** Present address: E.I. du Pont de Nemours & Co. CR and D, Exptl. Station, Wilmington, DE, U.S.A.

Abbreviations: APC, allophycocyanin; Chl, chlorophyll; CMC, critical micelle concentration; HPLC, high-performance liquid chromatography; MMCM, 20 mM Mes-NaOH/10 mM $MgCl_2$/20 mM $CaCl_2$/0.5 M Mannitol; PC, phycocyanin; PS, Photosystem; SB, sulfobetain; SDS-PAGE, SDS-polyacrylamide gel electrophoresis.

Correspondence: H.T. Witt, Max-Volmer-Institut für Biophysikalische und Physikalische Chemie, Technische Universität Berlin, Strasse des 17. Juni 135, 1000 Berlin 12, Germany.

Introduction

Photosystem II (PS II) performs the light-induced reduction of plastoquinone and oxidation of water, generating molecular oxygen. At least the primary photochemical activity of PS II is performed by two intrinsic membrane proteins called D-1 and D-2 (about 32 and 34 kDa), as has been proposed [1,2] on the basis of the similarity between PS II and the photosystem of purple bacteria. The recent isolation of a complex containing the D-1 and D-2 polypeptides and cytochrome *b*-559 [3,4], as well as the detection of primary PS II photochemistry in these preparations [3–6], has provided evidence for this idea. Closely associated with these reactioncenter polypeptides are two chlorophyll-binding polypeptides called CPa-1 and CPa-2 (about 47 and 43 kDa) (see Refs. 7 and 8 for reviews about the polypeptides of PS II), and a number of extrinsic polypeptides that are involved in the water-splitting process, very likely in an indirect manner. In cyanobacteria, these extrinsic polypeptides consist of a 34 kDa protein similar to the one isolated from higher plants [9,10] and probably of a low-molecular-weight protein [11]. The 17 and 23 kDa proteins of chloroplasts are not detected in cyanobacteria [9].

Information concerning the overall structure of the active, oxygen-evolving PS II complex is relatively rare. In a previous paper [12] we reported on the isolation and purification of highly active PS II complexes from the thermophilic cyanobacterium *Synechococcus* sp. The particles with molecular weights of about 300 and 500 kDa were attributed to monomeric and dimeric forms of PS II, respectively. From negative staining data we estimate dimensions of $15.5 \times 10.5 \times 6.5$ nm and $15 \times 18.5 \times 6.5$ nm for the oxygen-evolving PS II monomers and dimers, respectively, in the non-ionic detergent dodecyl β-D-maltoside [12].

In this contribution we present further details of the isolation procedure and characteristics of the oxygen-evolving PS II particles from *Synechococcus* sp. Estimations concerning the contributions of the extrinsic proteins and detergents to the size, shape and mass of these particles are given and a model for cyanobacterial PS II in vivo is presented.

Materials and Methods

The growth medium according to Ref. 13 was kept at 58° C and supported by air enriched with 4% CO_2. During the growth period (3–4 days), the amount of air was increased stepwise from 80 to 150 l/h and the illumination with white light was increased stepwise to a maximum of 15 000 lux.

The growing of the cells, membrane preparations, PS II extraction, and sucrose density gradient procedures resulting in the SG-1 and SG-2a and SG-2b complexes were carried out as outlined earlier in Refs. 12, 14, 15. To the first sucrose gradient SB 12 was added in concentrations varying from 0 to 0.06%. Due to this addition, the amounts of APC in the SG-1 fraction could be diminished drastically, but the yield of chlorophyll decreased in general. For each extract, the optimal SB 12 concentration was determined.

For Tris treatment, 2 parts of SB 12 extract were diluted with 1 part of 2.4 M Tris-HCl (pH 8.3) and incubated for 15 min in daylight at room temperature. With these fractions, the first and second sucrose gradients were performed as described above for the oxygen-evolving preparations, except that the Mes buffer was replaced by 100 mM Tris-HCl (pH 8.0). The resulting PS II preparations were designated SG-1T and SG-2T, respectively. All green fractions were frozen and stored at −80° C before further use.

SDS-polyacrylamide gel electrophoresis was carried out on 10–15% gradient acrylamide slab gels according to Laemmli [16]. Protein bands were stained with Coomassie brilliant blue. Oxygen evolution was measured either with a Clark-type electrode (Rank Brothers) or with a zirconium dioxide sensor [17] at room temperature using repetitive, single-turnover xenon flashes (repetition frequency 2 Hz). The reaction medium contained MMCM (see Ref. 12) at pH 6.5, 500 μM phenyl-*p*-benzoquinone, 1 mM ferricyanide and PS II diluted to about 10 μM Chl.

Reaction center concentrations of PS II were measured via flash-induced absorbance changes at 320 nm, which primarily indicate the turnover of the primary quinone acceptor, Q_A [18].

HPLC was performed on a Waters apparatus as described in Ref. 12. Size-exclusion chromatography (gel filtration) was done with a TSK 4000

SW column (Beckmann) and ion-exchange chromatography with a Mono-Q 5/5 column (Pharmacia). For all columns the flow medium was MMCM (pH 6.5) (see Ref. 12), supplemented by the amount of detergent indicated.

Specimens for electron microscopy were prepared by the droplet method, using uranyl acetate as a negative stain. Electron microscopy was carried out on a Philips electron microscope at 70 000 magnification. Selected micrographs were digitized with a Datacopy Model 610 F electronic digitizing camera [19].

Results

Sucrose gradients

Oxygen-evolving PS II was extracted from membranes of the thermophilic cyanobacterium *Synechococcus* sp. by the zwitterionic detergent SB 12, in principle as described by Schatz and Witt [14,15]. The preparations show a high oxygen-evolving activity and are largely depleted of PS I, but still contain relatively large amounts of the phycobilin pigment-proteins, PC and APC.

For the purification of oxygen-evolving PS II from these SB 12 extracts, a two-step procedure consisting of two successive sucrose gradients was developed. In the first sucrose gradient the concentration of the detergent SB 12 was kept below its CMC (0.1%), thus allowing the photosystem to aggregate. Under these conditions PS II migrates in a relatively sharp band in the lower part of the gradient (Fig. 1, inset), clearly separated from the PC and most of the APC pigments. Fig. 1 (full line) shows the absorbance spectrum of a typical PS II fraction (called SG-1) from such a gradient together with the spectrum of an SB 12 extract (dashed line). The decreased absorbance near 620 and 650 nm suggests that the SG-1 preparations are strongly depleted of PC and APC. The chlorophyll peaks are observed at 673 and 436 nm, the same wavelengths at which other PS II reaction center complexes show their absorbance maxima. The relatively high absorbance near 470 and 510 nm indicates that the SG-1-preparations contain more carotenoid than other reaction center complexes.

The second sucrose-gradient fractionation step is performed in the presence of detergent ((3–5) × CMC). With dodecyl β-D-maltoside as detergent, a fractionation as in the inset of Fig. 2 occurs in most cases. In the upper part of the gradient a yellow band is observed clearly separated from a middle (SG-2a) and a lower (SG-2b) green band.

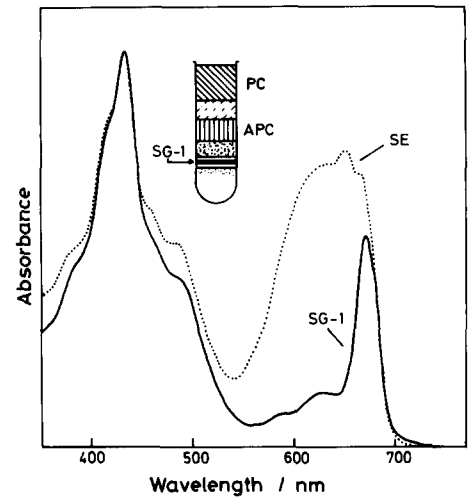

Fig. 1. Absorbance spectra of the SB 12 extract (dashed line) of an SG-1 preparation (solid line) after the first sucrose-gradient centrifugation. The arrow indicates the green PS-II-containing SG-1 fraction.

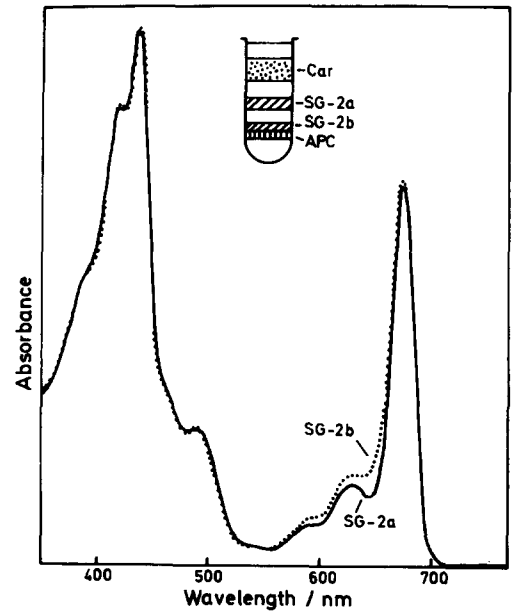

Fig. 2. Absorbance spectra of an SG-2a preparation (solid line) and of a typical SG-2b preparation (dashed line) after the second sucrose-gradient centrifugation.

Closely below or combined with the lower green band, a blue band is observed in some cases. Absorption spectra identified the upper yellow band with carotenoid and the lower blue band with APC. The absorption spectra of the green SG-2a and SG-2b bands are shown in Fig. 2. They are similar to that of the SG-1 preparation (Fig. 1, full line) except that the amount of carotenoid is considerably lower. While the upper green band SG-2a (Fig. 2, full line) is largely depleted of APC, the lower one, SG-2b (dashed line), cannot be separated well from APC and it still contains this pigment protein in most cases. In a few cases, the second sucrose gradient yielded a fourth band (SG-2x), located between the yellow carotenoid fraction and the SG-2a band (details, see below). This fraction contained chlorophyll peaking at 671 nm and carotenoid. The characteristic shoulder at 680 nm of PS II core complexes [20] was not observed.

When the first sucrose gradient was done with 100 mM Tris, (pH 8.0) instead of Mes buffer, a pattern similar to that in the inset of Fig. 1 was observed. However, the second sucrose gradient with this material yielded only one green band (SG-2T), at about the same position as SG-2a.

HPLC gel filtration

HPLC experiments were performed in order to obtain information about the homogeneity of the preparations. The SG-1 fractions eluated near the void volume (Fig. 3, solid line) which indicates a molecular weight of several millions. No smaller fractions were observed. This indicates that SG-1 fractions consist of large aggregates obviously due to the absence of detergents.

With detergent in concentrations above the CMC (both in the running buffer and in the applied sample) the peak in the void volume region disappeared concurrent with the appearance of three new fractions (Fig. 3, dashed line). This shows that the aggregation of the SG-1 preparation is reversible. The fractions of about 500 and 300 kDa were green and contained chlorophyll. The relative amplitudes of both varied considerably, the variation being dependent on the SB 12 extract used. The smallest fraction was yellow, contained carotenoid and migrated as 50–120 kDa particles. As purified β-carotene in dodecyl β-D-maltoside yielded a mass of about 100 kDa (not shown). This yellow fraction is very likely due to free carotenoid embedded in detergent micelles. Besides, no protein could be found upon performing SDS-PAGE.

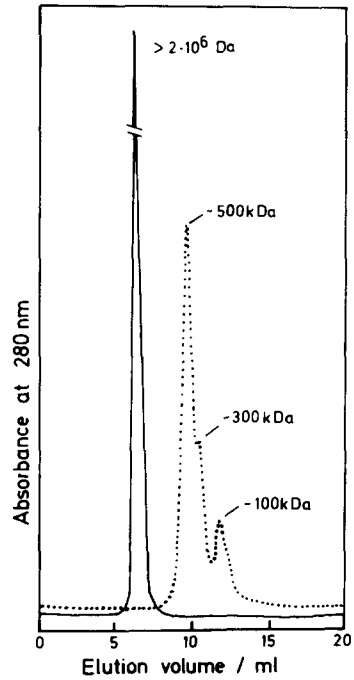

Fig. 3. Elution profile of an SG-1 preparation on a gel filtration column TSK 4000 SW in the absence of detergent (solid line) and in the presence of 0.03% β-DM (dashed line). Flow rate 0.5 ml/min.

Fig. 4 shows the relative amounts of the different fractions in the SG-1 preparations in dependence on the concentration of dodecyl β-D-maltoside. Similar results have been obtained with other detergents, i.e., SB 12, lysophosphatidylcholine and *n*-octyl β-D-glucopyranoside. In the region of the CMC there is a sharp turning point, but above the CMC the relative intensity of the free fractions remained constant, suggesting that the 500 kDa fraction is not a partial aggregation product of the smaller fractions. It has been shown before that the fractions from the second sucrose gradient, SG-2a and SG-2b consist of very pure 300 kDa and 500 kDa fractions, respectively [12]. Gel filtration experiments with the Tris-treated SG-2T fraction indicated a mass of 300 kDa. Isolated APC (the middle fraction from the first sucrose gradient) revealed many fragments, the

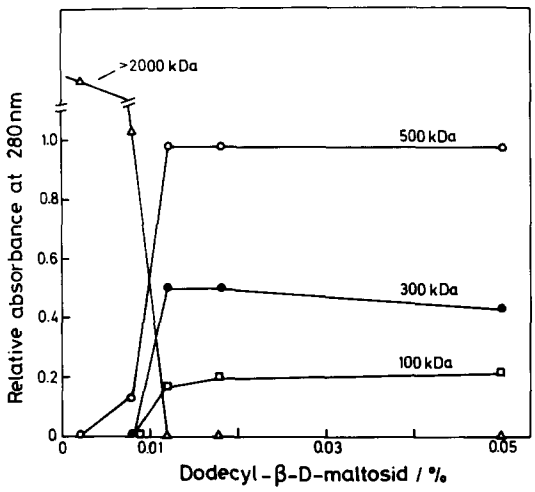

Fig. 4. Relative amplitude on the peaks shown in Fig. 3 in dependence on the concentration of dodecyl β-D-maltoside.

most prominent peaks being near 20 and 500 kDa. Together with the finding that APC-rich 500 kDa fractions showed exactly the same molecular mass as fractions with only trace amounts of APC, it shows that APC is not connected with the 500 kDa fraction but forms its own fraction with about the same mass. This explains the higher APC content of the 500 kDa fraction.

The exact mass of the '300' and '500' kDa fractions as determined by the gel-filtration HPLC column depends on the micelle diameter of the specific detergent used. Table I shows the mass of the '300' kDa SG-2a fraction determined with different detergents. These values have been checked, also, by using different gel filtration columns, which all yielded similar results (not shown). The lowest value was observed with *n*-octyl β-D-glucopyranoside, which indeed has the smallest micelle diameter of the detergent tested. Thus, the molecular mass values with *n*-octyl β-D-glucopyranoside should be the closest approach to the real masses of the complexes.

TABLE I

MOLECULAR MASS OF SG-2a FRACTION

Molecular mass of the oxygen-evolving '300' kDa SG-2a fraction in dependence on different detergents used on the gel-filtration column (TSK 4000 SW); the detergent concentration was 3×CMC in each case.

Detergent	Mass (kDa)
Dodecyl β-D-maltoside	300±10
LL	280±10
n-Octyl β-D-glucopyranoside	270±10
SB 12	310±10

The fraction SG-2x, which appeared in the second sucrose gradient in some cases, consisted of particles with an apparent mass of 150 kDa in dodecyl β-D-maltoside (not shown), which is only about 50 kDa more than the apparent mass of free β-carotene in dodecyl β-D-maltoside.

HPLC anion-exchange chromatography

Further purification could be obtained by ion exchange chromatography. We used an FPLC Mono-Q HR 5/5 column, equilibrated with Mes buffer (pH 6.5) in the presence of 0.03% dodecyl β-D-maltoside. The carotenoid micelles did not bind to the column, which was also the case for the aggregated SG-1 complexes. After solubilization, however, the PS II complexes bound to the column and could be eluted upon applying a gradient of 5–200 mM $MgSO_4$. SG-1 complexes yielded three main fractions at about 45, 60 and 65 mM $MgSO_4$ (not shown).

Fig. 5 shows the elution profiles of fractions from the second sucrose gradient on the Mono Q column. The 500 kDa SG-2b complexes gave one prominent peak at about 65 mM $MgSO_4$ (Fig. 5A, dashed line), while the 300 kDa SG-2a fraction showed two peaks at about 45 and 60 mM $MgSO_4$, respectively (Fig. 5A, solid line). Tris-treated SG-2T complexes had only one peak at 45 mM (Fig. 5B, solid line), while the trimeric PS I (Fig. 5B, dashed line) complex [21] was eluted at about 85 mM $MgSO_4$ with this method (see also Ref. 22).

SDS-PAGE

The polypeptide composition of the complexes was examined by SDS-polyacrylamide gel electrophoresis. Fig. 6A shows a densitometer scan of a typical SG-1 preparation. The main bands correspond to proteins with apparent masses of 51, 46, 35, 31 and 29 kDa. They may be attributed to proteins generally found in oxygen-evolving PS II complexes, i.e., the chlorophyll-binding proteins CPa-1 and CPa-2, the extrinsic 34 kDa protein and the reaction center proteins D_2 and D_1, respectively. The proteins at 19 and 17 kDa are

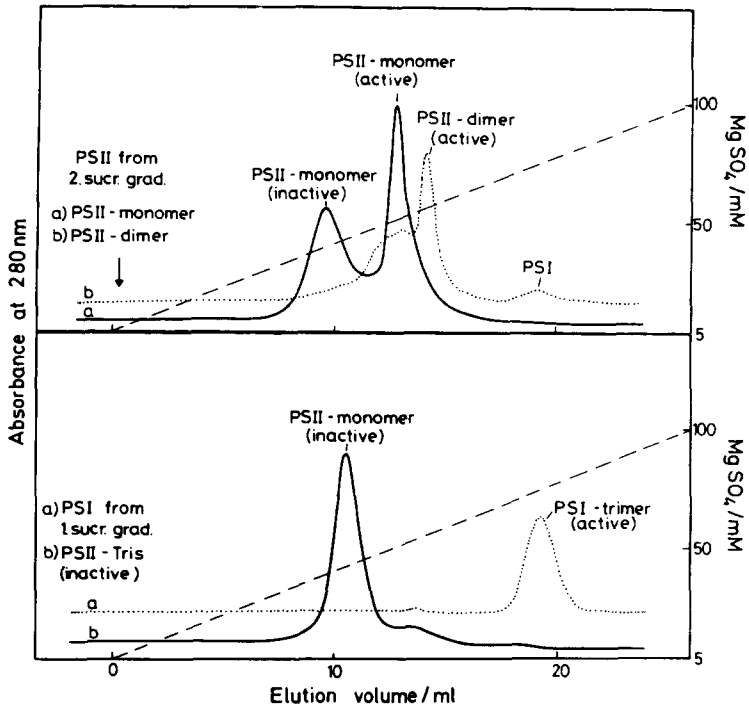

Fig. 5. Elution profiles of the SG-2a (a), SG-2B (b), SG-2T (b), and SG-1 of PS I (b) preparations on the anion-exchange column Mono Q HR-5/5. Flow rate 0.4 ml/min.

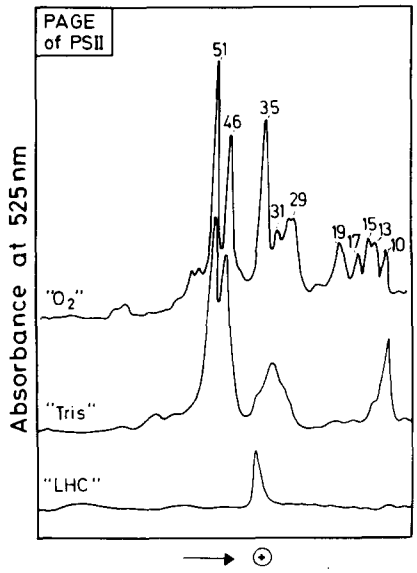

Fig. 6. Densitometer scan of SDS-polyacrylamide gels: (A) O_2 evolving SG-1 preparation; (B) Tris-treated SG-2 preparation (SG-2T); (B) 38 kDa fraction (SG-2x). The horizontal axis indicates the migration distances of the marker proteins.

attributed to a residual contamination by APC and the faint bands at 120/110 kDa, as well as part of the stain at about 29 kDa may be attributed to PS II-APC linker proteins or fragments of it. The small absorption at 64/59 kDa can be due to PS I [21] or to the α- and β-subunits of the F_1-ATPase complex, respectively. The proteins at around 15, 13 and 10 kDa are probably due to PS II, since their intensities correlated with those of the PS II proteins upon comparison of different preparations, and not with those of the APC and/or linker proteins. They are probably due to cytochrome *b*-559 and other low-molecular-weight proteins of the oxygen-evolving complex [11]. The SG-2a complex is more purified and lacks the APC/linker/PS I/ATPase contaminations [12]. The Tris-treated SG-2T complex in addition lacks the 35 kDa extrinsic protein and probably also the proteins at 15 and 13 kDa (Fig. 6B). The same was found for the fraction at 45 mM from SG-2a after the Mono-Q column (Fig. 5A). Surprisingly, SG-2x

TABLE II

FLASH YIELDS AND Q_A

Average O_2 flash yields and amounts of photoreducible Q_A in the different PS II preparations. SB 12, SG-1, -2a and -2b are taken from Ref. 12.

	$\frac{1}{4}O_2$/Chl	Q_A/Chl
SB 12 extract	1/(70±20)	1/(60±20)
SG-1 1st centrifugation	1/(60±10)	1/(50±10)
SG-2a 2nd centrifugation	1/(80±30)	1/(45±5)
SG-2b 2nd centrifugation	1/(80±30)	1/(45±5)
SG-2a Mono Q isolation at 60 mM	1/(50±10)	1/(33±2)
SG-2a Mono Q isolation at 45 mM	–	1/(40±2)
SG-1T 1st centrifugation	–	1/(50±10)
SG-2T 2nd centrifugation	–	1/(45±5)
SG-2x 2nd centrifugation	–	–

gave only one peak at 35 kDa (Fig. 6C), i.e., exactly the same mass as the extrinsic 35 kDa protein involved in oxygen evolution. When the samples were incubated before electrophoresis at 15°C instead of 37°C, however, it migrated at 38 kDa and had a green color, indicating that the protein is different from the extrinsic protein and is involved in chlorophyll binding.

Photochemical activities

Table II shows the oxygen-flash yields and the amount of photoreducible Q_A in the preparations (the values for the SB 12 extract and SG-1, 2a and 2b have been reported already in Ref. 12). For the SG-1 preparations the capacity of oxygen evolution and of Q_A reduction is increased by about 20% in general, which may be due to the loss of some inactive chlorophyll. The capacity of Q_A reduction was even slightly higher in both the SG-2a and SG-2b preparations for which routinely values between 40 and 50 Chl/Q_A were found. Although both SG-2a and SG-2b showed considerable water-oxidizing activity, oxygen evolution appeared to be less stable in these preparations. This may be due to the loss of carotenoid and the use of detergent. The stability appeared to be strongly dependent on the type of detergent used. After Tris treatment, the capacity to evolve oxygen was lost, but the amount of Q_A reduction remained unchanged (Table II).

On the Mono Q column, the SG-2a fraction separated into two fractions which eluted at 45 and 60 mM $MgSO_4$, resp. (see above). The fraction at 60 mM showed a distinct increase in O_2-evolving activity, while the fraction at 45 mM was completely inactive. Both showed a very high reaction-center activity as indicated by the amount of photoreducible Q_A. Therefore, the fraction at 60 mM represents the normal, O_2-evolving PS II particle, while the fraction at 45 mM represents those PS II complexes without O_2-evolving capacity. The absence of the extrinsic protein(s) would then be the cause for the changed behavior on the anion exchange column. Care was taken to determine the optimal reaction center activity in the active part of the SG-2a fraction which eluted with 60 mM $MgSO_4$ from the Mono Q column. With five different preparations a number of 31 Chl *a* molecules per Q_A was found. It was checked by SDS-PAGE that the polypeptide composition was normal, i.e., that the intensity of the apoproteins of the chlorophyll-binding complexes CPa-1 and CPa-2 was not changed.

The SG-2x complex was neither active in oxygen evolution nor able to show photoreduction of Q_A (Table II). Measurements at 820 nm in the nanosecond time range, indicating the turnover of the primary electron donor Chl-a_{II} (P-680), revealed neither the characteristic 11 ns decay at the Chl-a_{II}^+/Pheo$^-$ radical pair [23] in closed centers nor the slower phases [5,6]. Also, the slower kinetics of Chl-a_{II}^+ forward electron transfer were not recorded (Schlodder, E., unpublished data). Very likely, the 35 kDa apoprotein of SG-2x is not involved in PS II photochemistry but is, instead, the apoprotein of a light-harvesting complex.

Electron microscopy

The preparations were negatively stained with uranyl acetate and analyzed by electron microscopy. In the SB 12 extracts most of the PS II molecules were aggregated into long strings with a length of up to several 100 nm, as shown in Fig. 7A. The numerous top views of cylindrical particles with a diameter of 11–12 nm are phycobilisome fragments and consist of PC and/or APC. Under the applied sample preparation conditions no interaction between these cylinders and the strings was found. In the SG-1 preparations these

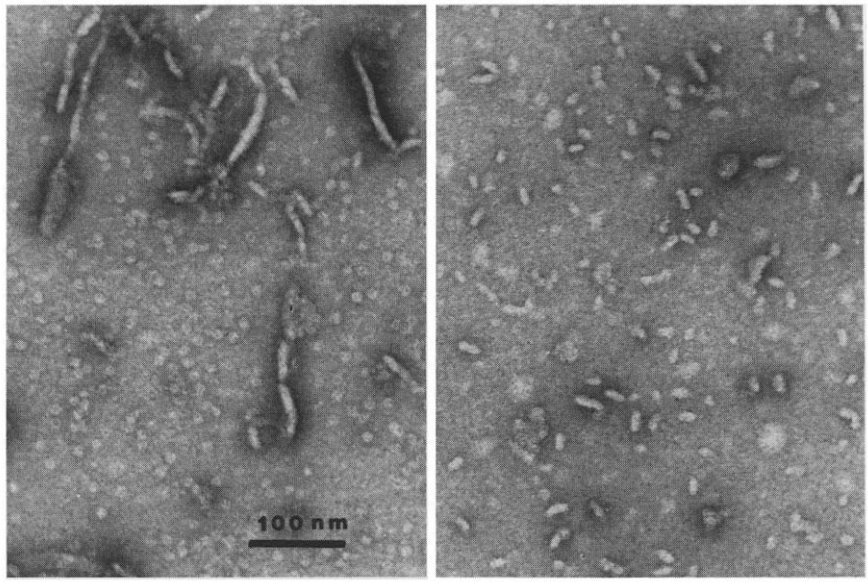

Fig. 7. (A) Electron micrograph of the SB 12 extracts, showing PS II particles in string-like aggregates andphycobilisomes fragmented into cylindrical parts. (B) SG-1 PS II particles diluted with buffered 0.15% SB 12. Specimens were negatively stained with 1% uranyl acetate.

cylindrical fragments were virtually absent, confirming the loss of phycobilisome components. Without detergent, very large, vesicle-like aggregates were observed (not shown). With higher detergent concentrations (3–5-times CMC), electron micrographs as in Fig. 7b were routinely obtained, showing relatively small particles without aggregated structures.

More information is gained by analysis of the SG-2T, SG-2a and SG-2b preparations which consist of homogeneous 300 and 500 kDa (SG-2b) particles, resp. It has been shown before [12] that the SG-2a and -2b preparations consist of one type of particle in mainly two projections: a top and a side view. Upon preparation for electron microscopy both the 300 and 500 kDa particles frequently aggregate in such a way that the side view is seen as the repeating unit. Tris-treated SG-2T particles aggregate in a similar way (not shown), suggesting that the lost extrinsic 34 kDa protein is not responsible for this phenomenon. Interestingly, there is always a small but clear gap of 1.3 ± 0.3 nm between the individual molecules in the aggregates. The dimensions of the Tris-treated SG-2T complexes are given in Table III, together with the dimensions of SG-2a and -2b from Ref. 12. The center-to-center distance of the individual particles in the 'roll'-like aggregates was also measured. While the smallest dimension (about 6.5 nm) is identical for the oxygen-evolving 300 and 500 kDa fractions, it seems to be slightly smaller in the Tris-treated material, suggesting a contribution from the extrinsic 34 kDa protein to this dimension in the oxygen-evolving particles.

TABLE III

PARTICLE DIMENSIONS

Dimensions of oxygen-evolving PS II particles (500 and 300 kDa) taken from Ref. 12) and Tris-treated 300 kDa PS II particles prepared in 0.15% dodecyl β-D-maltoside. Dimensions measured from electron micrographs. *a*, length of rods and discs; *b*, width of discs; *c*, width of rods; *d*, center-to-center distance in roll-like aggregates. Standard deviation indicated for all measurements.

	500 kDa	300 kDa	(Tris) 300 kDa
a	18.5 ± 1.0 nm ($n = 127$)	15.8 ± 0.8 nm ($n = 144$)	15.5 ± 0.8 ($n = 50$)
b	15.5 ± 1.4 nm ($n = 49$)	10.5 ± 0.8 nm ($n = 51$)	10.9 ± 0.6 ($n = 14$)
c	6.6 ± 0.6 nm ($n = 56$)	6.4 ± 0.7 nm ($n = 54$)	5.6 ± 0.5 ($n = 30$)
d	8.0 nm	7.6 nm	7.0 nm

This contribution is supposed to be about 1 nm, as indicated by the difference in center-to-center distance between the dimers and the Tris-treated monomers. The active monomers show an intermediate center-to-center distance which may be due to a greater part of particles inactive in O_2 evolution within this fraction. Concerning the other dimensions, the oxygen-evolving (SG-2a) and Tris-treated (SG-2T) 300 kDa fractions are very similar.

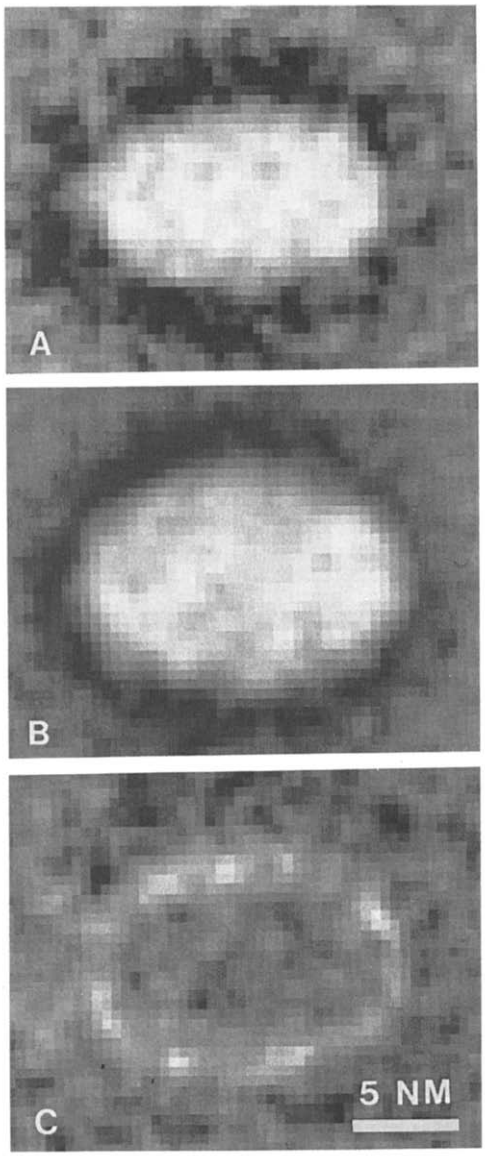

Fig. 8. Averaged images of PS II particles: (A) Averaged image of 32 top views of the 300 kDa particle in *n*-octyl β-D-glucopyranoside. (B) Averaged image of 106 top view projections of the 300 kDa particle prepared in β-DM (see ref. 12). (C) Difference image between (B) and (A).

Fig. 8 shows averaged top view projections of the 300 kDa fractions, solubilized with two different detergents. In case of the 300 kDa particles solubilized with dodecyl β-D-maltoside (Fig. 8B), a total of 106 of these projections was selected from two micrographs in arrays of 64×64 pixels (see also Ref. 12). As micrographs for image analysis, we used those that were already published in Ref. 12. The only criterion for selection was that the projections were well stained and not in contact or overlapping with other projections. The projections were brought into the same positions by alignment procedures and averaged by summation. Although the sum shows no internal features, the outlines are relatively sharp, as should be expected for the average of a population of homogeneous particles. The dimensions of this projection are 23×33 pixels or 10×15 nm. This is in accordance with the dimensions measured in enlarged prints (Table III).

In order to investigate the contribution of detergent, we analyzed top views of 300 kDa particles in *n*-octyl β-D-glucopyranoside, which has a considerably smaller micelle diameter than dodecyl β-D-maltoside. Micrographs used for the image analysis correspond to those presented in Ref. 12 for dodecyl β-D-maltoside (not shown). Fig. 8A shows the sum of 32 views, resulting in slightly smaller particles (18×31 pixels or 8.5×14.5 nm) than those in Fig. 8B. The difference between them is depicted in Fig. 8C.

Discussion

Our previous report [12] and this paper describe the isolation and purification of oxygen-evolving and Tris-treated PS II complexes from the thermophilic cyanobacterium *Synechococcus* sp. The particles have polypeptide compositions similar to those of other, purified 'core complexes' from PS II [24–29] and show activities that are among the highest reported up to now for such complexes: reaction center activities of one photoreducible Q_A per 33 ± 2 Chl molecules and O_2 flash yields of $1/4$ O_2 per 50 ± 10 Chl molecules were measured for the most active fraction after

the anion-exchange chromatography step. In a few cases, depending on the growth of the cyanobacteria another green complex could be observed in addition to the monomeric and dimeric PS II complexes. This complex, called SG-2x in this paper, showed a molecular mass of about 150 kDa (not shown) upon performing gel filtration and consists of only one apoprotein with an apparent mass of about 35 kDa. Under non-denaturing conditions, it migrated at about 38 kDa and kept at least part of its green color. It is tempting to speculate that this protein corresponds to the one reported by Sherman and co-workers [30] to accumulate under Fe^{2+}-deficient growth conditions. Under these circumstances, phycobilisome function is impaired and the newly synthesized protein could be involved in taking over the light-harvesting function. The apparent absence of any reaction center activity is consistent with this idea. These results raise serious questions about the suggestion of Worland et al. [31] that a 38 kDa protein is the D_2 reaction center protein in *Synechococcus*.

The HPLC analysis of the two O_2-evolving PS II fractions, SG-2a and SG-2b, from the second sucrose gradient has shown that both are homogeneous, consisting of about 300 and 500 kDa particles, respectively [12]. This property allowed a detailed analysis of the shape of the particles by electron microscopy. Both the 300 and 500 kDa particles have the shape of a discoid object and appear mainly in two projections. Based on the dimensions from Fig. 8 and Table III, the 500 kDa particle is about 1.8-times larger than the 300 kDa one [12]. We have, however, to account for additional detergent and lipid binding to the protein. HPLC-experiments (Table I) and electron micrographs (Fig. 8) clearly showed a correlation between the molecular weight and the micelle diameter of the detergent used for solubilization. If we assume a boundary layer of 1.5 nm for dodecyl β-D-maltoside attached to the hydrophobic parts of the protein in the top views, the volume would be about 20% smaller. With these corrected dimensions the molecular mass of the 300 and 500 kDa fractions would be 220–270 kDa and 440–540 kDa, respectively, assuming a value of $2.0 \pm 0.2 \cdot 10^{-3}$ nm^3/Da [32]. This confirms our former conclusion (see Ref. 12) that the 300 kDa particle represents the monomeric form and the 500 kDa one a dimeric form of PS II.

Information about the in vivo orientation of the elliptical discs in the thylakoid membranes is gained from a comparison of the shape and dimensions of the 300 kDa particles in dodecyl β-D-maltoside and *n*-octyl β-D-glucopyranoside (Fig. 8). Since *n*-octyl β-D-glucopyranoside molecules are much smaller (about 1 nm in length) than dodecyl β-D-maltoside, the difference between both (Fig. 8) suggests that the detergent is evenly distributed in a boundary layer around the molecules in the top view projection. Therefore, the outer protein regions in this projection must be rather hydrophobic.

Concerning the inner protein region, information is gained from the type of roll-like aggregates that are especially predominant in the 500 kDa fraction [12]. Stain accumulation in the small but clear gap of 1.3 nm between individual molecules strongly suggests that it separates rather hydrophilic parts of the molecules. The gap itself can be explained by assuming small subunit protrusions extending from the surface of the molecules that hinder closer contact. These observations suggest that in vivo the PS II particles are oriented with their long axis parallel to the plane of the membrane, extending up to 8 nm (6.4–6.6 nm plus protrusions) across the membrane.

This view on the orientation of the PS II particles in the thylakoid membranes is supported by the 300 kDa particle prepared after Tris treatment. This particle has the same top view dimensions as the oxygen-evolving 300 kDa particle but a smaller side-view dimension (about 5.8 nm instead of 6.5 nm in O_2-evolving complexes – Table III). Since after Tris treatment the extrinsic 34 kDa polypeptide is missing, it is reasonable to assume that this subunit is responsible for the different thickness.

Among the different kinds of aggregate observed in the electron micrographs (Figs. 7 and 8 and Ref. 12) the roll-like aggregation of the particles as in Ref. 12 is probably artefactual and induced by the preparation of the samples for electron microscopy. The localization of the phycobilisome at one of the hydrophilic sites excludes such an in vivo organization. On the other hand, the long strings observed in the SB 12

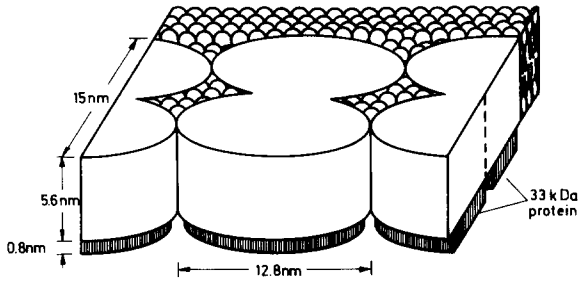

Fig. 9. Model for the structure of cyanobacterial PS II complexes and its arrangement in the membrane according to the results of the electron micrographs in Ref. 12.

extracts (Fig. 7a) may reflect the in vivo organization of PS II, since the organization of the PS-II-bound phycobilisomes in long rows is well documented [33,34]. As the strings disappear upon addition of detergent, they seem to be stabilized by hydrophobic interaction.

More stable is the kind of aggregation formed by the dimers, since higher concentrations of mild detergents like dodecyl β-D-maltoside are not able to break these structures (Fig. 4). Tris treatment, on the other hand, results in pure monomers, suggesting hydrophilic factors for the maintenance of the dimers. However, treatment with 1 M $MgSO_4$ (which does not inhibit oxygen evolution) has no influence on the amount of dimers (not shown) suggesting a specific Tris effect and not a general salt effect. Maybe the removal of the 34 kDa extrinsic polypeptide is a prerequisite for salts and detergents to attack the binding region between the dimers.

A proposal for the structural organization of cyanobacterial PS II in vivo is shown in Fig. 9. According to Manodori and Melis [25] twice as many PS II complexes as phycobilisomes exist in cyanobacteria. Therefore, it seems likely that the dimers represent the normal, functional PS II present in the thylakoid membranes [12]. When the phycobilisomes occur in rows in vivo, it is likely that PS II occurs in double rows. A similar conclusion has been drawn before [36] after freeze-etching studies. Recently, Mörschel and Schatz [37] reorted freeze-etching and negative-staining data on membranes and PS II particles from *Synechococcus* sp., and evidence was given for the double-row organization of PS II in this organism (Fig. 9). Their data suggest top-view dimensions of roughly 10×10 nm for the PS II monomer, which corresponds relatively well to our estimations. Their statement, however, that the longest dimension (13.5 nm) is perpendicular to the membrane cannot be accounted for with our data. Maybe the presence of linker protein and/or APC in the particles of Mörschel and Schatz can explain the observed differences.

In cyanobacteria like *Synechococcus* sp. the phycobilisomes are hemidiscoidally shaped with a height of about 30 nm, a width of about 60 nm, and a thickness of about 10 nm [38]. Presumably, they are oriented perpendicular on the top of the long strings in Fig. 9. The size of the PS II complexes suggests that the repeating unit in the strings is 12.5–13 nm. As a result, the distance between the individual phycobilisomes in the rows should be the same and can be used as a test for the reliability of the model in Fig. 9. Mörschel and Möhlethaler [39] reported a periodicity of 12 nm in membranes of the thermophilic cyanobacterium *Mastigocladus laminosus,* and Mörschel and Schatz [37] found the same distance in *Synechococcus* sp. These data strongly support the model of Fig. 9.

Acknowledgements

We gratefully acknowledge the financial support provided by the Deutsche Forschungsgemeinschaft (Sonderforschungsbereich 312) and also wish to thank Ms. D. DiFiore and I. Geisenheimer for their excellent technical assistance.

References

1 Michel, H. and Deisenhofer, J. (1986) in Photosynthesis III, Photosynthetic Membranes and Light Harvesting Systems (Staehelin, L.A. and Arntzen, C.J., eds.), pp. 371–381, Springer Verlag, Berlin.
2 Trebst, A. (1986) Z. Naturforsch. 41c, 240–245.
3 Nanba, O. and Satoh, K. (1987) Proc. Natl. Acad. Sci. USA 84, 109–112.
4 Barber, J., Chapman, D.J. and Telfer, A. (1987) FEBS Lett. 220, 67–73.
5 Danielius, R.V., Satoh, K., Van Kan, P.J.M., Plijter, J.J., Nijs, A.M. and Van Gorkom, H.J. (1987) FEBS Lett. 213, 241–244.
6 Takahashi, Y., Hansson, Ö., Mathis, P. and Satoh, K. (1987) Biochim. Biophys. Acta 893, 49–59.
7 Ghanotakis, D.F. and Yocum, C.F. (1985) Photosynth. Res. 7, 97–114.

8 Satoh, K. (1985) Photochem. Photobiol. 42, 845–853.
9 Stewart, A.C., Ljungberg, U., Akerlund, H.-E. and Andersson, B. (1985) Biochim. Biophys. Acta 808, 353–362.
10 Koike, H. and Inoue, Y. (1985) Biochim. Biophys. Acta 807, 64–73.
11 Stewart, A.C., Siczkowski, M. and Ljungberg, U. (1985) FEBS Lett. 913, 175–179.
12 Rögner, M., Dekker, J.P., Boekema, E.J. and Witt, H.T. (1987) FEBS Lett. 219, 207–211.
13 Castenholz, R.W. (1969) Bacteriol. Rev. 33, 476–504.
14 Schatz, G.H. and Witt, H.T. (1984) Photobiochem. Photobiophys. 7, 1–14.
16 Schatz, G.H. and Witt, H.T. (1984) Photobiochem. Photobiophys. 7, 77–89.
16 Laemmli, U.K. (1970) Nature (London) 227, 680–685.
17 Schlodder, E. and Meyer, B. (1987) Biochim. Biophys. Acta 890, 23–31.
18 Stiehl, H.H. and Witt, H.T. (1968) Z. Naturforsch. 24b, 1588–1598.
19 Boekema, E.J., Berden, J.A. and Van Heel, M.G. (1986) Biochim. Biophys. Acta 851, 353–360.
20 Van Dorssen, R.J., Plijter, J.J., Dekker, J.P., Den Ouden, A., Amesz, J. and Van Gorkom, H.J. (1987) Biochim. Biophys. Acta 890, 134–143.
21 Boekema, E.J., Dekker, J.P., Van Heel, M.G., Rögner, M., Saenger, W., Witt, I. and Witt, H.T. (1987) FEBS Lett. 217, 283–286.
22 Witt, I., Witt, H.T., Gerken, S., Saenger, W., Dekker, J.P. and Rögner, M. (1987) FEBS Lett. 221, 260–264..
23 Schlodder, E. and Brettel, K. (1988) Biochim. Biophys. Acta 933, 22–34.
24 Ikeuchi, M. and Inoue, Y. (1986) Arch. Biochem. Biophys. 247, 97–107.
25 Franzén, L.G., Styring, S., Etienne, A.-L., Hansson, Ö. and Vernotte, C. (1986) Photobiochem. Photobiophys. 13, 15–28.
26 Ghanotakis, D.F., Demetriou, D.M. and Yocum, C.F. (!() Biochim. Biophys. Acta 891, 15–21.
27 Yamada, Y., Tang, X.-S., Itoh, S. and Satoh, K. (1987) Biochim. Biophys. Acta 891, 129–137.
28 Ohno, T., Satoh, K. and Katoh, S. (1986) Biochim. Biophys. Acta 852, 1–8.
29 Satoh, K., Ohno, T. and Katoh, S. (1985) FEBS Lett. 180, 326–330.
30 Bullerjahn, G.S., Riethman, H.C. and Sherman, L.A. (1985) Biochim. Biophys. Acta 810, 148–157.
31 Worland, S.T., Yamagishi, A., Isaacs, S., Sauer, K. and Hearst, J.E. (1987) Proc. Natl. Acad. Sci. USA 84, 19774–19778.
32 Matthews, B.W. (1968) J. Mol. Biol. 33, 491–497.
33 Staehelin, L.A. (1986) in Photosynthesis III, Photosynthetic Membranes and Light Harvesting Systems (Staehelin, L.A. and Arntzen, C.J., eds.), pp. 1–84, Springer Verlag, Berlin.
34 Manodori, A. and Melis, A. (1985) FEBS Lett. 181, 79–82.
36 Giddings, T.M., Wassman, C. and Staehelin, L.A. (1983) Plant Physiol. 71, 409–419.
37 Mörschel, E. and Schatz, G.H. (1987) Planta 172, 145–154.
38 Gantt, E. (1986) in Photosynthesis III, Photosynthetic Membranes and Light Harvesting Systems (Staehelin, L.A. and Arntzen, C.J., eds.), pp. 260–268, Springer Verlag, Berlin.
39 Mörschel, E. and Mühlethaler, K. (1983) Planta 158, 451–457.